*Scientia Africana, Vol. 22 (No. 1), April, 2023. Pp 29-40* *https://dx.doi.org/10.4314/sa.v22i1.4*
*© Faculty of Science, University of Port Harcourt, Printed in Nigeria* *ISSN 1118 – 1931*

# LITHOLOGIC CHARACTERIZATION OF IGUOSA EROSION SITE USING GEOELECTRICAL TECHNIQUES

**[1]Egbo, D.O. and [2]Airen, O.J.**
[1,2] Department of Physics, Faculty of Physical Sciences, University of Benin, Nigeria.
Corresponding author E-mail: okeegbo@gmail.com

*Received: 13-02-2023*
*Accepted: 02-04-2023*

## ABSTRACT

*Considering the devastating menace of gully erosion for which lithology is one amongst several other agents that drives soil loss and gully erosion, Vertical Electrical Sounding (VES) and Electrical Resistivity (ERT) techniques were adopted to investigate subsurface lithology in Iguosa gully erosion site. PASI 16GL model resistivity meter was used in acquiring data for VES and ERT in the area under investigation. VES data acquired were processed both qualitatively and quantitatively, and geoelectric sections were generated using AUTOCAD software by combination of two or more interpreted VES results along a profile. ERT data were processed using Res2dinv software to an inverse model resistivity section. The geoelectric image generated were interpreted to obtain lithology of the subsurface. The analysis and interpretation of the subsurface image reveals presence of topsoil, sand, dry sand, clayey sand and coarse sand. The subsurface lithology within the study location is predominantly sandy. The result obtained from the resistivity of all profiles shows that erodibility increases with depth within this study area with corresponding high resistivity values. Due to the fact that sand within the study area is loose coarse and silty, whilch can give rise to high resistivity and causes erosion.*

**Keywords:** Geoelectric, Subsurface, Sand, Erodibility and Res2dinv

## INTRODUCTION

The global society exists and thrives upon the earth's surface. The raw materials for economic activities and human existence are derived from the subsurface such as rocks, naturally occurring minerals and water found in earth's surface. It is important to consider the geologic make up of an area in the construction of buildings, highways, hydropower station and dams (Egbo and Bright, 2020). Lithological mapping is important parameters for interpreting, identifying and mapping of minerals (Tripathi *et al.*, 2019). Lithological mapping in an area defines the characteristic nature of rock types and their associated formation. Since lithology is concerned with the physical properties of rock, the lithology of coastline affects the speed at which it erodes. Lithology and rock structure play a vital role in the development of drainage network in any drainage basin. The drainage patterns upon land surface develop according to the underlying lithology and rock structure (Sucheta and Vibhash, 2011). Generally, soil loss and gully erosion in particular are driven by lithology, climate change, land use and land cover change amongst many other factors (Omran *et al.*, 2019). It is found that most gullies occur in unconsolidated materials, including colluvium and alluvium, deeply weathered substrates or aeolian deposits such as loosed formations (Maerker *et al.*, 2008; Frankl *et al.*, 2012).

Geophysical methods respond to the physical properties of the subsurface media (e.g., electrical resistivity, density, porosity, seismic

velocity, etc.) and can be applied successfully when some physical properties in a region differs sufficiently from another. One of the many direct ways in which geophysical investigation aids the general economy (e.g., natural resources, environmental remediation, infrastructure, renewable energy and agriculture) is in the delineation of subsurface lithology or rock types (Ezomo and Ifedili, 2005). The use of geophysical techniques continues to increase from the conventional application in natural resource exploration to civil engineering, rock mechanics, disaster prevention, environmental preservation, among others as a result of the geological model that is generated from the geophysical data (Takahashi *et al.,* 2006; Knödel *et al.,* 2007).

The distribution of electrical resistivity within the subsurface is delineated by injecting current into the ground and measuring the resulting potential difference V. Conventionally, this is done either by profiling which measures lateral variation of electrical resistivity in the subsurface or vertical electrical sounding (VES) which measures vertical variation of resistivity. Electrical resistivity tomography (ERT) technique is a combination of profiling and VES which has become the preferred choice for near surface investigations. Subsurface cavities have also been surveyed to assess the likelihood of landslides in an area with the ERT (Panek *et al.,* 2010). Lithological classifications obtained from integrated geophysical and geological mapping of lithology and geologic structures correlates well with drill logs (Aning *et al.,* 2019). Electrical resistivity tomography was applied to investigate subsurface soil electrical properties. This effectively indicated two different lithology with high resistivity in the top soil and low resistivity below. High resistivity suspected as pyroclastic deposit with a lot of volcanic rocks fragment and the low resistivity suspected to be volcanic deposit with high – saturated water indicative of clay (Fattah *et al.,* 2019). Emenike and Chetty (2022) investigated the internal structure and groundwater characterization of a landslide site in Nanka, Anambra State, Nigeria using resistivity technique. The results of the study reveal that the study area is mainly clayey and sandstone formation with mostly low resistivity values corresponding to the shale layers and groundwater zones. Babaiwa and Airen, (2021) used Electrical Resistivity Tomography (ERT) to investigate erosion site in Auchi Edo State Nigeria. The results revealed that the subsurface is underlain by topsoil, lateritic sand, sand and sandstone. The high resistivity distributions above 1000 Ωm observed are indications of vulnerabilities of the study area to erosion. Karim and Tucker-Kulesza, (2018) carried out an investigation using Electrical Resistivity Tomography in predicting soil erodibility. The results of this study reveal that an ER over 50 Ωm has a 93% probability of classifying the soil as high erodibility.

The objective of this study is to map the lithology in Iguosa and environs, using Electrical Resistivity Tomography and Vertical Electrical Sounding to gain a detailed understanding of the continued gully erosion menace in the study area.

## Geology of the Study Area

The study area (Figure 1) occupies the Southern part of Edo State which is underlain by sedimentary formation whose geology falls under Benin Formation of the Niger Delta Basin. The formation consists of top reddish clayey sand capping highly porous fresh water bearing loose pebbly sands, sand and sandstone with local thin clays and shale inter-

*Scientia Africana, Vol. 22 (No. 1), April, 2023. Pp 29-40* https://dx.doi.org/10.4314/sa.v22i1.4
*© Faculty of Science, University of Port Harcourt, Printed in Nigeria* *ISSN 1118 – 1931*

beds which are considered to be of braided stream origin. It is characterized by deposits laid during Tertiary and Cretaceous periods (Reyment, 1965). The Benin Formation locally covered with Quaternary drift (loose brownish sand) varies in thickness but attains a maximum thickness of 6000ft (approx. 1970m) near the sea shore. The sedimentary rock contains about 90% of sand stone and shale intercalations (Alile *et al.*, 2011). Edo State is situated in South-western part of Nigeria. It is an important sedimentary basin in Nigeria due to her closeness to the oil fields within the Niger-Delta region.

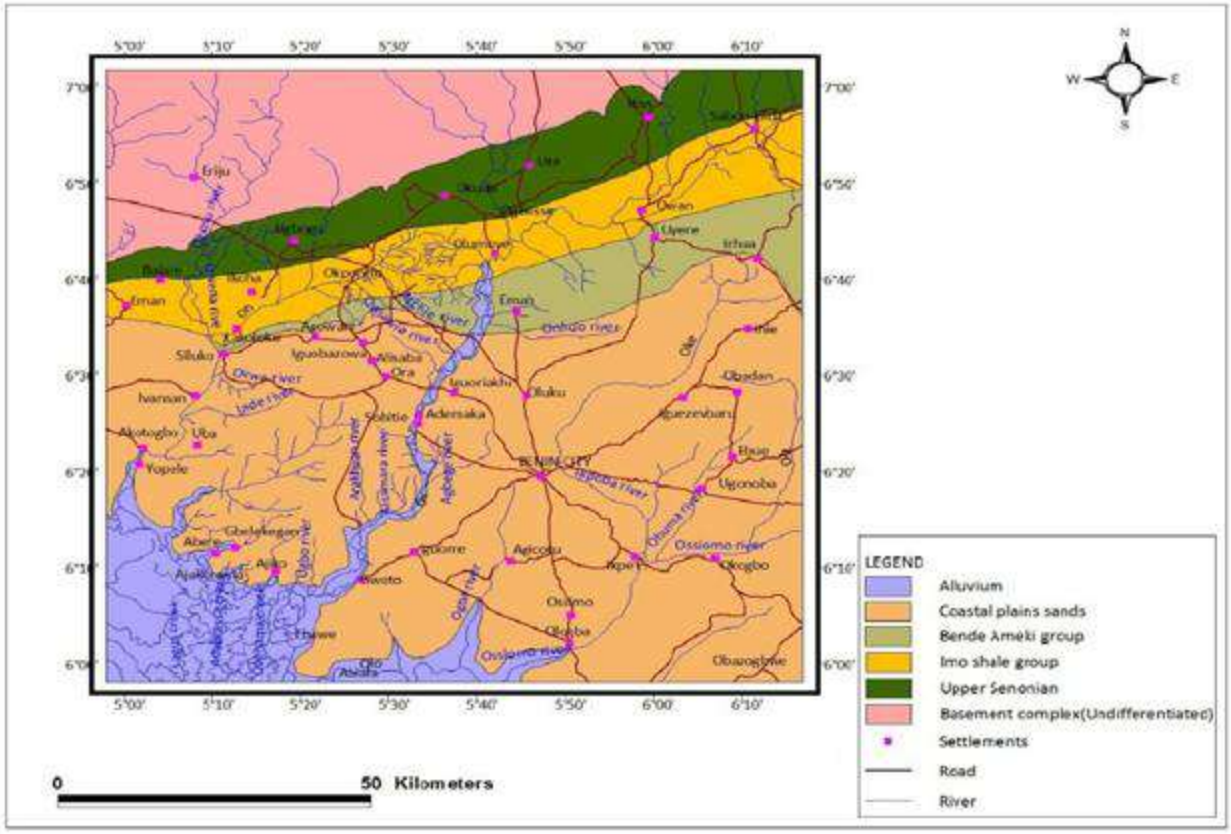


**Figure 1: Map of Edo State showing the study area (Olatunji et al., 2014)**

## MATERIALS AND METHODS

The geophysical survey was carried out in Iguosa gully erosion site located in Ovia North East Local Government Area, with Longitudes 005° 36' 35.54" E to 005° 36' 38.63" E, latitudes 06° 27' 07.18" N to 06° 27' 02.60" N and elevation of 50 to 49 m. These coordinates were obtained using Garmin 12 Global positioning system (GPS). Schlumberger and Wenner electrode configurations were employed for VES and ERT respectively. The Schlumberger electrode–configuration was employed with current electrode separation (AB) varied from a minimum of 2 to 160 m. A total of twelve (12) VES stations were acquired. Wenner electrode configuration with electrode spacing varied from minimum of 10m to 60m was employed. A total of four (4) ERT traverses were acquired. Electrodes were coupled with the ground using the hammer till good contact was made to the ground. The current and voltage electrodes were connected

to the resistivity meter via the reels of electric cables using alligator clips so as to ensure firm and good connection. The investigation of lithology was carried out by injecting current *I* into the subsurface and the corresponding values of the resistance were read off on the PASI 16GL resistivity meter and recorded. The cables were checked after each VES and ERT data was acquired to ensure cables are not damaged which can affect data quality.

Electrical Resistivity Tomography data acquired was processed using Res2dinv software and a 2D resistivity image for each traverse was obtained which represents the true subsurface resistivity. Vertical Electrical Sounding data acquired were processed both qualitatively and quantitatively. Partial curve matching technique was used in the interpretation of the depth sounding curves quantitatively (Bhattacharya and Patra, 1968)**.** Accordingly, the VES data points were plotted on a transparent paper. The partial curve matching technique employed the use of a standard two (2) layer master curves and four (4) auxiliary type curves (H, K, A, and Q). This procedure required segment-by-segment curve matching starting from the position with shorter electrode spacing and moving towards those with longer spacing. The WinResist software was adopted in the interpretation of the survey data. VES curves were obtained from the partial curve matching and then used to constrain the interpretation by this computer software. This invariably reduces overestimation of depths in the curve matching. The result of the computer iteration quantitatively reveals the resistivity, thickness and depth. Qualitatively, depth sounding curves interpretation was carried out based on individual geo-electric characteristics on the number of layers represented by the four types of the auxiliary curves (A, H, K, and Q) and also from the profiles and maps involving the inspection for patterns/anomaly signatures that are diagnostic of the lithostrategraphy. Geoelectric sections were generated using AUTOCAD software by combining two or more interpreted VES results along a profile.

Using these techniques, acquired data were processed and the resistivity imaging were interpreted geologically using the standard resistivity values for rocks, minerals and sediments from available literatures and also using the knowledge of the local geology of the research area.

## RESULTS AND DISCUSSION

The results obtained from the interpreted VES within the study area

**Table 2: Summary of the interpreted VES results with inferred lithology**

| | **IGUOSA EROSION SITE** | | | | | |
|---|---|---|---|---|---|---|
| **VES No** | **LAYERS** | **RESISTIVITY (Ωm)** | **THICKNESS (m)** | **DEPTH (m)** | **CURVE TYPE** | **LITHOLOGY** |
| 1 | 1 | 223.0 | 0.7 | 0.7 | **A** | Topsoil |
| | 2 | 233.9 | 9.1 | 9.8 | $\rho_1 < \rho_2 < \rho_3$ | Sand |
| | 3 | 3551.8 | --- | --- | | Coarse Sand |
| 2 | 1 | 175.9 | 0.6 | 0.6 | **HK** | Topsoil |
| | 2 | 90.2 | 5.6 | 6.3 | $\rho_1 > \rho_2 < \rho_3 > \rho_4$ | Clayey Sand |
| | 3 | 1783.4 | 10.0 | 16.3 | | Coarse Sand |
| | 4 | 792.6 | --- | --- | | Sand (Saturated) |
| 3 | 1 | 137.2 | 0.7 | 0.7 | **AA** | Topsoil |
| | 2 | 156.0 | 4.8 | 5.5 | $\rho_1 < \rho_2 < \rho_3 < \rho_4$ | Clayey Sand |

*Scientia Africana, Vol. 22 (No. 1), April, 2023. Pp 29-40* https://dx.doi.org/10.4314/sa.v22i1.4
*© Faculty of Science, University of Port Harcourt, Printed in Nigeria* *ISSN 1118 – 1931*

| | | | | | | |
|---|---|---|---|---|---|---|
| | 3 | 326.4 | 15.0 | 20.5 | | Sand |
| | 4 | 2138.1 | --- | --- | | Coarse Sand |
| 4 | 1 | 3232.7 | 0.8 | 0.8 | **HA** | Topsoil |
| | 2 | 631.9 | 6.5 | 7.3 | $\rho_1 > \rho_2 < \rho_3 < \rho_4$ | Sand |
| | 3 | 1659.9 | 19.5 | 26.8 | | Sand (Dry) |
| | 4 | 5903.3 | --- | --- | | Coarse Sand- |
| 5 | 1 | 2512.2 | 0.6 | 0.6 | **HK** | Topsoil |
| | 2 | 818.5 | 4.7 | 5.3 | $\rho_1 > \rho_2 < \rho_3 > \rho_4$ | Sand |
| | 3 | 4117.3 | 13.8 | 19.1 | | Coarse Sand |
| | 4 | 736.4 | --- | --- | | Sand (Saturated) |
| 6 | 1 | 1440.8 | 0.6 | 0.6 | **HK** | Topsoil |
| | 2 | 475.1 | 4.1 | 4.8 | $\rho_1 > \rho_2 < \rho_3 > \rho_4$ | Sand |
| | 3 | 2804.9 | 17.7 | 22.4 | | Coarse Sand |
| | 4 | 549.3 | --- | --- | | Sand (Saturated) |
| 7 | 1 | 116.3 | 0.6 | 0.6 | **HA** | Topsoil |
| | 2 | 84.4 | 4.6 | 5.2 | $\rho_1 > \rho_2 < \rho_3 < \rho_4$ | Clayey Sand |
| | 3 | 306.5 | 15.0 | 20.2 | | Sand |
| | 4 | 908.8 | --- | --- | | Sand |
| 8 | 1 | 78.6 | 0.6 | 0.6 | **HA** | Topsoil |
| | 2 | 47.4 | 3.1 | 3.8 | $\rho_1 > \rho_2 < \rho_3 < \rho_4$ | Clay |
| | 3 | 286.8 | 17.7 | 21.5 | | Sand |
| | 4 | 2693.7 | --- | --- | | Coarse Sand |
| 9 | 1 | 118.3 | 0.6 | 0.6 | **HA** | Topsoil |
| | 2 | 73.3 | 4.0 | 4.6 | $\rho_1 > \rho_2 < \rho_3 < \rho_4$ | Clayey Sand |
| | 3 | 388.8 | 15.2 | 19.8 | | Sand |
| | 4 | 4173.5 | --- | --- | | Coarse Sand |
| 10 | 1 | 576.6 | 0.5 | 0.5 | **HA** | Topsoil |
| | 2 | 100.7 | 2.4 | 2.9 | $\rho_1 > \rho_2 < \rho_3 < \rho_4$ | Clayey Sand |
| | 3 | 1095.5 | 20.4 | 23.3 | | Sand (Dry) |
| | 4 | 2326.5 | --- | --- | | Coarse Sand |
| 11 | 1 | 906.8 | 0.8 | 0.8 | **HA** | Topsoil |
| | 2 | 229.0 | 4.8 | 5.6 | $\rho_1 > \rho_2 < \rho_3 < \rho_4$ | Clayey Sand |
| | 3 | 601.2 | 13.8 | 19.3 | | Sand |
| | 4 | 2026.5 | --- | --- | | Coarse Sand |
| 12 | 1 | 3208.0 | 0.8 | 0.8 | **HA** | Topsoil |
| | 2 | 689.9 | 7.1 | 7.9 | $\rho_1 > \rho_2 < \rho_3 < \rho_4$ | Sand |
| | 3 | 1070.5 | 14.5 | 22.4 | | Sand (Dry) |
| | 4 | 9328.3 | --- | --- | | Coarse Sand |

By combining two or more interpreted VES stations from Table 2, the goelectric sections were generated.

**Geoelectric Section along MM' and NN'**

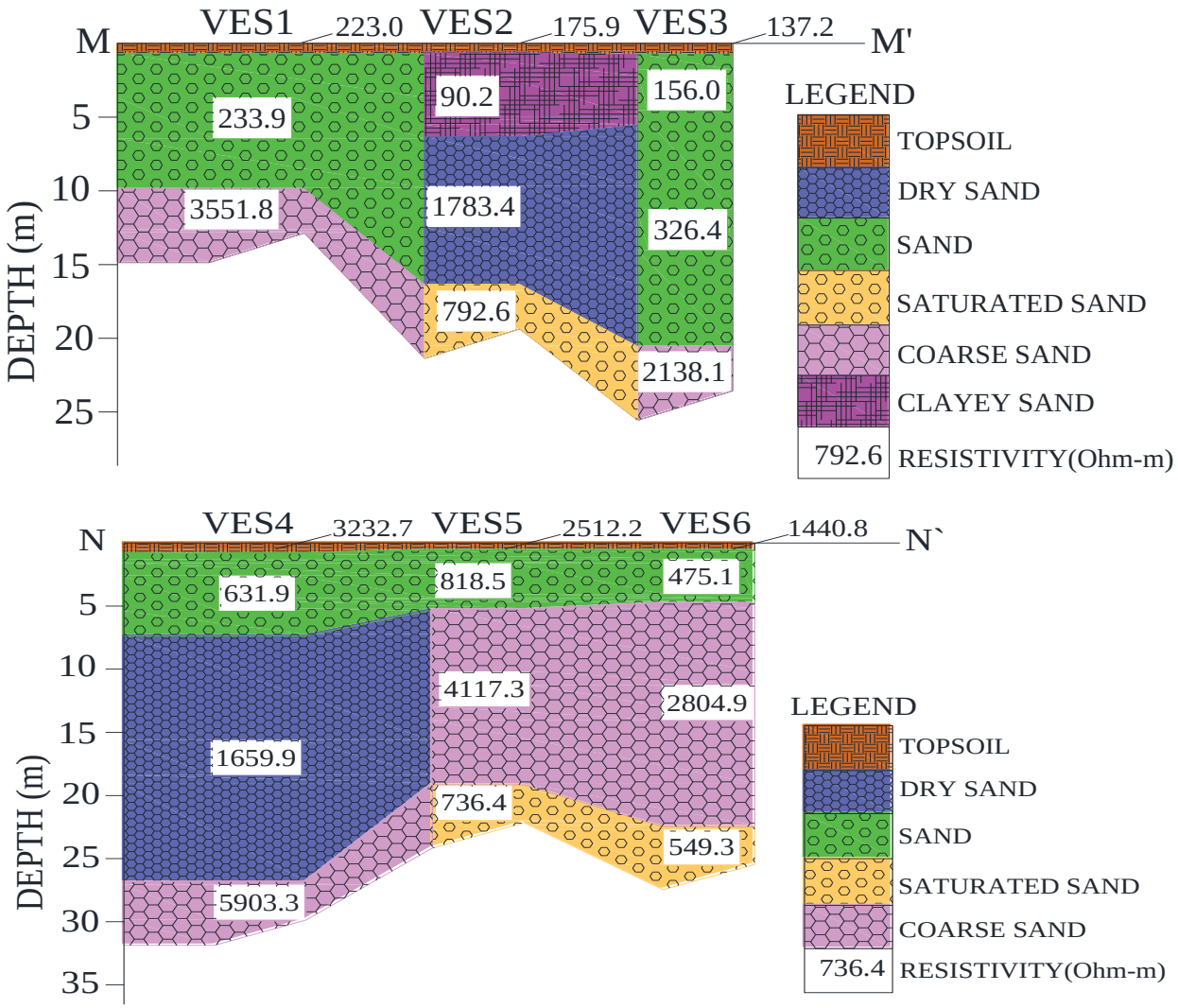


**Figure 10: Geoelectric Section for VES 1 to 6.**

**Geoelectric Section along OO' and PP'**

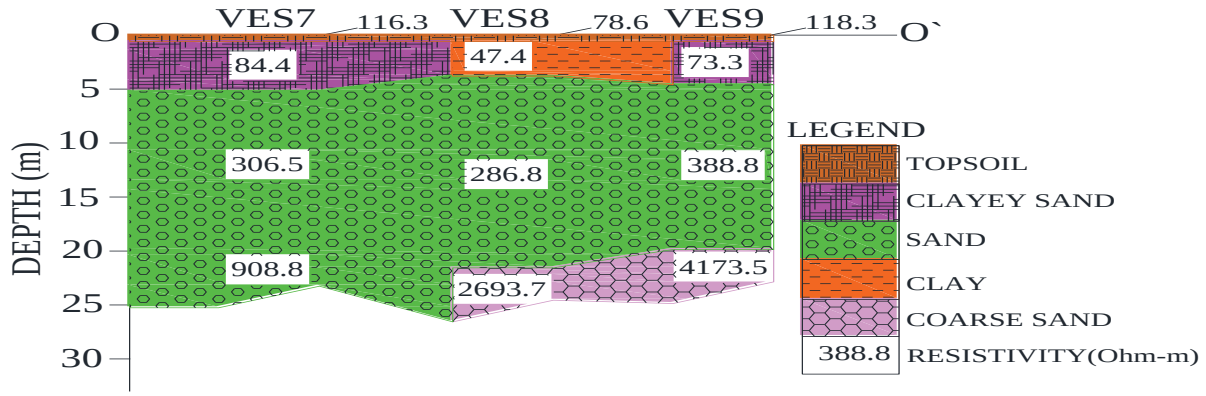

*Scientia Africana, Vol. 22 (No. 1), April, 2023. Pp 29-40* https://dx.doi.org/10.4314/sa.v22i1.4
*© Faculty of Science, University of Port Harcourt, Printed in Nigeria* *ISSN 1118 – 1931*

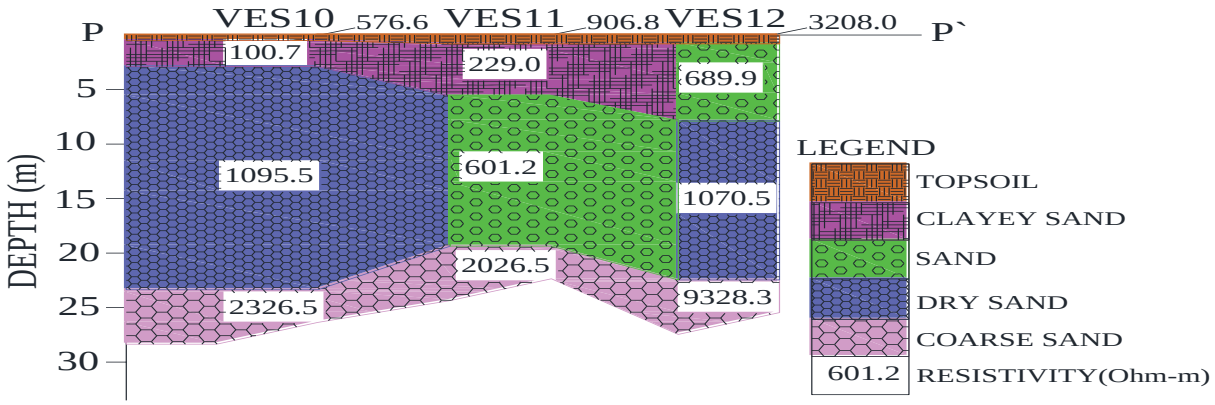


**Figure 11: Geoelectric Section for VES 7 to 12.**

The results from the VES (1 to 12) shows that the subsurface reveals three to four geoelectric layers which is underlain by the topsoil, clay, clayey sand, coarse sand, dry sand, saturated sand and sand (Figures 10 and 11). The topsoil is characterized by resistivity values ranging from 78.6 to 3208.0 ohm-m and layer thickness of 0.5 to 0.8 m. The second horizon connote clay, clayey sand and sand with resistivity values ranging from 47.4 to 818.5 ohm-m and layer thickness of 2.9 to 9.1 m. The third layer is representative of sand, dry sand and coarse sand having resistivity values ranging from 286.8 to 4117.3 ohm-m. The fourth substratum is diagnostic of sand, coarse sand and saturated sand with resistivity values ranging from 549.3 to 9328.3 ohm-m but their layer thickness could not be determined because the current terminated with in the region. High near-surface resistivity values of the resistivity structures are indicative of dry and unconsolidated geologic earth materials which are highly erodible (Karim and Tucker-Kulesza, 2018; Karim *et al*., 2019). The near-surface along VES 4, 5, 6 and 12 are thus suspected to be prone to erosion due to distributions of the high resistivity values. The coarse sand and dry sand, are due to its localized and unconsolidated nature which can also cause erosion (Figures 10 and 11).

## 2-D Resistivity Section along Traverse 1 – 4.

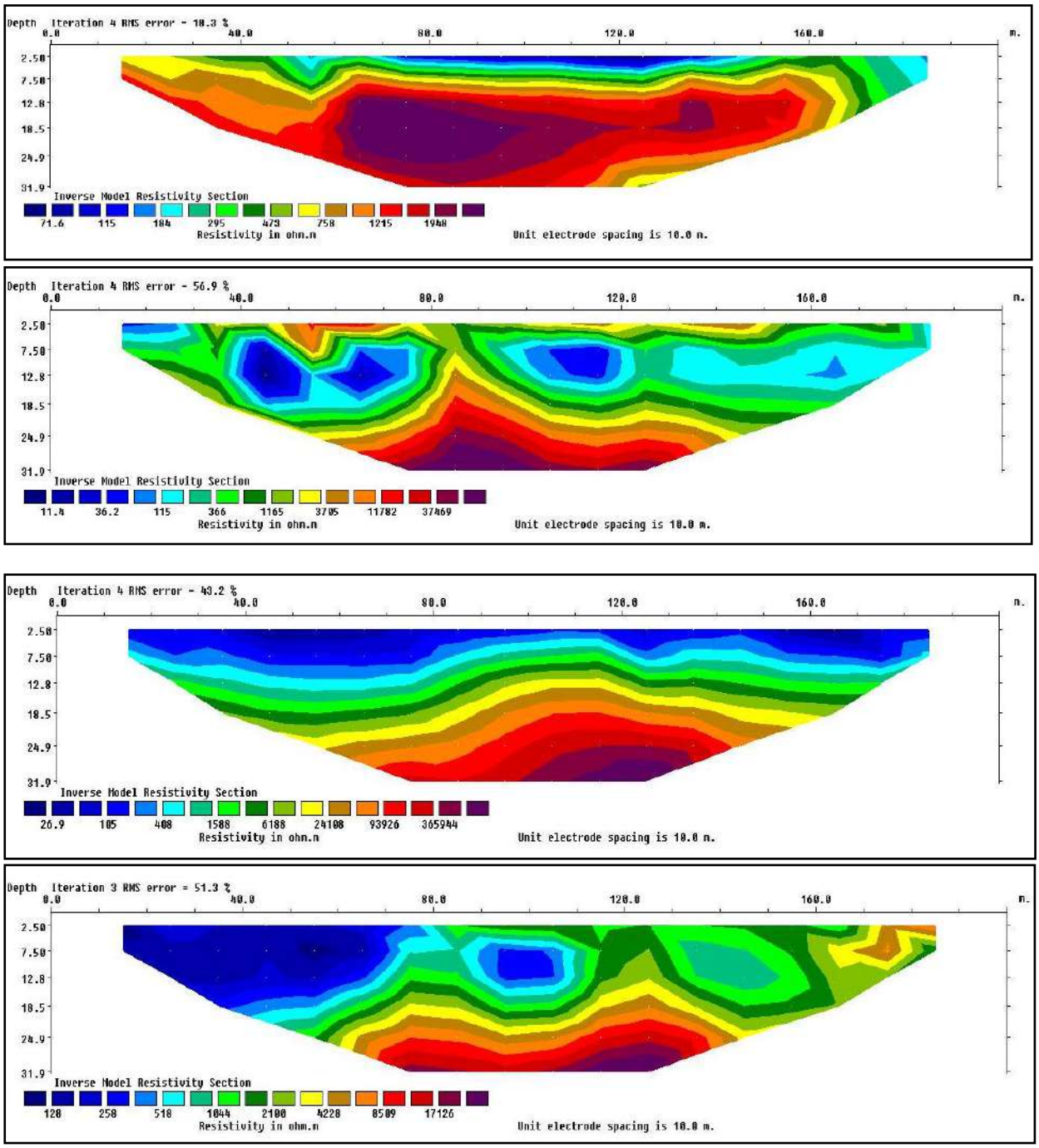


**Figure 12: 2-D Electrical Resistivity Structure Along Traverse (1 to 4).**

The 2D resistivity subsurface image along traverse 1 to 4 (Figure 12) delineates two to three geoelectric zones marked by varrying resistivity values ranging from 11.4 to 365944 ohm-m and indicated by the different color ranges which are representative of topsoil, clay, clayey sand, dry sand and sandstone. The topsoil has resistivity value ranging from 128 ohm-m 473 ohm-m. The clayey sand has resistivity values ranging from 71.6 to 295 ohm-m. The dry sand has resistivity values ranging from 1215 to 24100 ohm-m while the clay has resistivity values of 11.4 to 31.9 ohm-m. The saturate sand has resistivity values

*Scientia Africana, Vol. 22 (No. 1), April, 2023. Pp 29-40* https://dx.doi.org/10.4314/sa.v22i1.4
*© Faculty of Science, University of Port Harcourt, Printed in Nigeria* *ISSN 1118 – 1931*

ranging from 472 to 756 ohm-m while the sandstone has resistivity values of 37469 to 365944 ohm-m. The resistivity information along this profile shows that the erodibility increases with depth within this study area. The high near-surface resistivity values of the resistivity structures are indicative of dry and unconsolidated geologic earth materials which are highly erodible (Karim *et al.*, 2019).

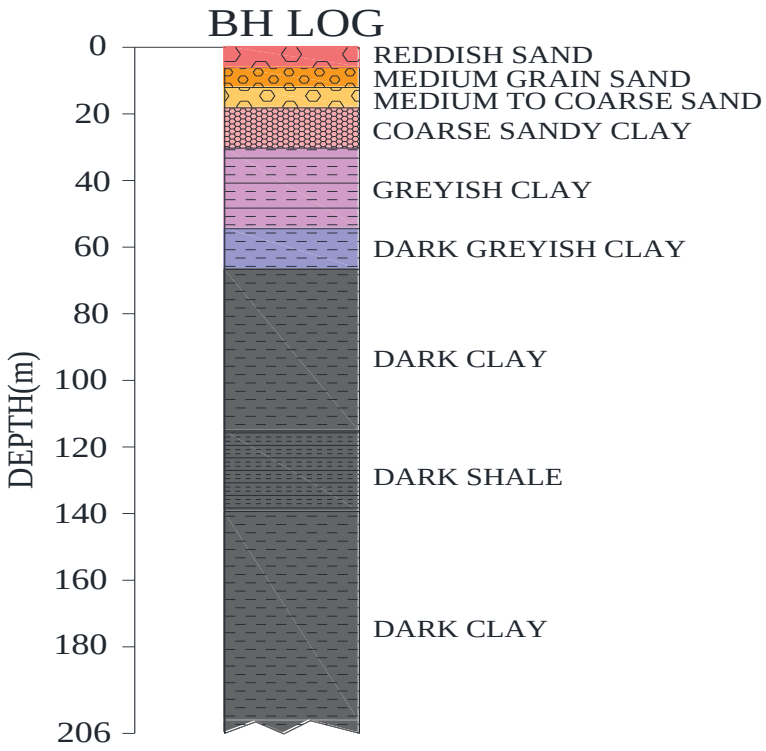


**Figure 13: Borehole Log Around the study area**

## CONCLUSION

The subsurface lithology in Iguosa has been delineated by adopting Wenner array configuration of electrical resistivity methods. Data acquired from each traverse in the area under investigation were processed using Res2dinv software. The geoelectric imaging generated were interpreted to obtain lithology of the subsurface. The analysis and interpretation from subsurface imaging reveals presence of topsoil, dry sand, saturated sand, clayey sand and coarse sand. The subsurface lithology within the study location is predominantly sand and shows erodibility of soil within the study area. The 2-D resistivity images also revealed that the resistivity increases with depth within the study area.

The study showed that erosion with intense scouring because of the high resistivity values near the surface and beneath the subsuface geology. The scouring depth ranges from 0 to 2 m and 12 – 31.9 m respectively. From this study it was determined that geoelectrical methods can be used to identify areas prone to erosion, so that authorities can use the information provided to take immediate action to stop or quell this threat.

**Acknowledgements**

My appreciation goes to Mr. Toafik Adeleke for his unreserved assistance during field data acquisition exercise for this study.

## Conflict of Interest

This research work did not in any way or whatsoever receive grants/funds from any organization, institution or agency.

## REFERENCES

Alile, O. M., Ujuanbi, O. and Evbuomwan, I. A. (2011). Geoelectric investigation of groundwater in Obaretin – Iyanomon locality, Edo state, Nigeria. Journal of Geology and Mining Research, 3(1), pp. 13 – 20.

Aning, A. A., Asare, V. S., Wemegah, D. D., Noye, R. M., Preko, K. and Danuor, S. K. (2019). Integrated Geophysical and Geological Mapping of the Lithological and Geological Structures at a Proposed Generator Site. Journal of Geoscience and Environment Protection, 7, 73-85. https://doi.org/10.4236/gep.2019.712005

Babaiwa, D. A. and Airen, O.J. (2021). Electrical Resistivity Tomography (ERT) for the Investigation of Erosion site in Oredide Village, Auchi in Etsako West LGA of Edo State, Southern Nigeria. *Journal of Applied Sciences and Environmental Management*, Vol. 25(5) pp. 887 – 891, DOI: 10.4314/jasem. v25i5.31

Bhattacharya, A.P.K. and Patra, H.P. (1968). *Direct Current Geoelectric Sounding: Principles and Interpretations: Methods of Geochemistry and Geophysics.* Elsevier Publishing Company, Amsterdam. 135.

Egbo, O. and Abanum. C. B. (2020). Lithostratigraphic Characterization of the Subsurface in Ologbo Community using Wenner-Schlumberger Electrode Configuration of Electrical Resistivity Method. International Journal of Advances in Scientific Research and Engineering (IJASRE), ISSN:2454-8006, DOI: 10.31695/IJASRE, 6(6), 46–56. https://doi.org/10.31695/IJASRE.2020.33830

Emenike, E.C. and Chetty, N. (2022). Use of Electrical Resistivity Tomography in investigating the internal structure of a landslide and its groundwater characterization (Nanka Landslide, Anambra State, Nigeria. *Jornal of Applied Science and Engineering (Taiwan)*, 25(4):

Ezomo, F. O. and Ifedili, S. O. (2005). Determination of water bearing formations at Osasogie Quarters by electrical Resistivity method. Journal of civil and Environ. Systems Engr. 6(1), 1-12.

Fattah, E., Paembonan, A., Suhendi C., Gultaf H., Rahmanda V., Augustina L., Saputra H., Sudibyo M., and Rizki, Reza (2019). Lithology Identification Using Electrical Resistivity Tomography Case Study: OAL's Construction Site. 3. 12-14.

Frankl A., Poesen J., Deckers J., Haile M. and Nyssen J. (2012). Gully head retreat rates in the semi-arid highlands of Northern Ethiopia. Geomorphology, 173, 185-195.

Karima, M. Z., Tucker-Kuleszaa, S. E. and BernhardtBarry, M. (2019). Electrical resistivity as a binary classifier for bridge scour evaluation. Trans Geotech; 19:146-157

Karim, M.Z. and Tucker-Kulesza, S.E. (2018). Predicting soil erodibility using electrical resistivity tomography. *Journal of Geotechnical Geo-environmental Engineering*;144(4):04018012. https://doi.org/10.1061/(ASCE)GT.1943-5606.0001857

Knödel, K., Lange, G., and Voigt, H. J. (2007). Environmental Geology: Handbook of Field Methods and Case Studies. Berlin: Springer Science & Business Media.

*Scientia Africana, Vol. 22 (No. 1), April, 2023. Pp 29-40* *https://dx.doi.org/10.4314/sa.v22i1.4*
*© Faculty of Science, University of Port Harcourt, Printed in Nigeria* *ISSN 1118 – 1931*

https://doi.org/10.1007/ 978-3-540-74671-3

Maerker M., Paz Castro C., Pelacani S. and Soto Bauerle M.V. (2008). Assessment of Soil Degradation Susceptibility in The Chacabuco Province of Central Chile Using a Morphometry Based Response Units Approach. Geografia Fisica e Dinamica Quaternaria, 31 (1), 47-53.

Olatunji, A. S., Asowata, T. I. and Abimbola, A. F. (2014). Geochemical Evaluation of Metal Content of Soils and Dusts of Benin City Metropolis, Southern Nigeria. J Geol Geosci 3:160

Omran, A., Maerker, M and Hochschild, V. (2019). Assessment of Gully Erosion in Relation to Lithology in the Southwestern Zagros Mountains, Iran Using Aster Data, GIS and Stochastic Modeling. Geografia Fisicae Dinamica Quaternaria. 41. 95 104. 10.4461/ GFDQ.2018.41.15.

Panek, T., Margielewski, W., Taborik, P., Urban, J., Hradecky, J. and Szura, C. (2010). Gravitationally Induced Caves and Other Discontinuities Detected by 2D Electrical Resistivity Tomography: Case Studies from the Polish Flysch Carpathians. Geomorphology, 123, 165-180. https://doi.org/10.1016/j.geomorph. 2010.07.008

Reyment, R.A. (1965). Aspects of the Geology of Nigeria, Ibadan University Press

Sucheta, M. and Vibhash, J. (2011). Role of Lithology and Rock Structure in Drainage Development in the Kaliani River Basin, Assam, India. Ethiopian Journal of Environmental Studies and Management. 4. 10.4314/ejesm.v4i2.7.

Takahashi, T., Takeuchi, T., and Sassa, K. (2006). International Society for Rock Mechanics Commission on Application of Geophysics to Rock Engineering-Suggested Methods for Borehole Geophysics in Rock Engineering. International Journal of Rock Mechanics and Mining Sciences, 43, 337-368. https://doi.org/10.1016/j.ijrmms.2005.09. 003

Tripathi, M., Govil, H. and Diwan, P. (2019). Lithological Mapping using Digital Image Processing Techniques on Landsat 8 OLI Remote Sensing Data in Jahajpur, Bhilwara, Rajasthan. 2nd International Conference on Intelligent Communication and Computational Techniques (ICCT), Jaipur, India, pp. 43-48, doi:10.1109/ICCT46177.2019. 8969043.